OPEN

Citation: Cell Death and Disease (2014) 5, e1440; doi:10.1038/cddis.2014.323

www.nature.com/cddis

Severe influenza A(H1N1)pdm09 infection induces thymic atrophy through activating innate CD8$^+$CD44^{hi} T cells by upregulating IFN-γ

B Liu[1,8], X Zhang[2,8], W Deng[3,8], J Liu[4], H Li[1], M Wen[2], L Bao[3], J Qu[1], Y Liu[1], F Li[3], Y An[2], C Qin*[,3], B Cao*[,1] and C Wang*[,1,5,6,7]

Thymic atrophy has been described as a consequence of infection by several pathogens including highly pathogenic avian influenza virus and is induced through diverse mechanisms. However, whether influenza A(H1N1)pdm09 infection induces thymic atrophy and the mechanisms underlying this process have not been completely elucidated. Our results show that severe infection of influenza A(H1N1)pdm09 led to progressive thymic atrophy and CD4$^+$CD8$^+$ double-positive (DP) T-cells depletion due to apoptosis. The viruses were present in thymus, where they activated thymic innate CD8$^+$CD44^{hi} single-positive (SP) thymocytes to secrete a large amount of IFN-γ. Milder thymic atrophy was observed in innate CD8$^+$ T-cell-deficient mice (C57BL/6J). Neutralization of IFN-γ could significantly rescue the atrophy, but peramivir treatment did not significantly alleviate thymic atrophy. In this study, we demonstrated that thymic innate CD8$^+$CD44^{hi} SP T-cells have critical roles in influenza A(H1N1)pdm09 infection-induced thymic atrophy through secreting IFN-γ. This exceptional mechanism might serve as a target for the prevention and treatment of thymic atrophy induced by influenza A(H1N1)pdm09.
Cell Death and Disease (2014) **5,** e1440; doi:10.1038/cddis.2014.323; published online 2 October 2014

Influenza A virus can cause recurrent epidemics and is the cause of one of the most important diseases, resulting in substantial human morbidity and mortality. The recent swine-origin 2009 pandemic influenza A H1N1 virus (influenza A(H1N1)pdm09) lead more than 60 million laboratory-confirmed cases in 214 countries and over 18 449 deaths until August 2010.[1] However, the basis for the increased pathogenesis of the virus remains not fully clear.

Although influenza A(H1N1)pdm09 did not cause high mortality, there was an unusually high frequency of fatal cases in healthy young and middle-aged patients.[2–4] More than 60% of the confirmed cases occurred in individuals between 5 and 29 years of age.[5] In addition to severe pathological pneumonia and hypercytokinemia in the lungs and serum,[2,6] we also previously found another hallmark of H5N1 or H1N1 virus infection in humans, which was strong reduction in T lymphocytes, also known as lymphopenia.[7–10] Peripheral lymphopenia occurs in parallel with thymic atrophy. Several microorganisms can infect the thymus and perturb the systemic T-cell pool.[11] Lymphopenia in fatal influenza A(H1N1)pdm09 cases in the young population may also be related to thymic atrophy.[12] Several mechanisms have been implicated in infection-induced thymic atrophy, and vary depending on the microorganism. Thymic atrophy in HPAIV infection has been reported to interfere with T-lymphocyte development through negative selection and glucocorticoids (GCs).[13,14] However, the mechanisms of influenza A(H1N1)pdm09-induced thymic atrophy have not been completely elucidated.

Unlike conventional T cells, which acquire effector function in the periphery following interaction with Ag,[15,16] some innate CD8$^+$ thymocytes in thymus display an effector-memory phenotype and effector function 'from birth' by rapidly producing cytokines upon stimulation.[16,17] A large proportion of innate CD8$^+$ thymocyte were found and developed in the thymus of Itk$^{-/-}$/RLK$^{-/-}$, KLF2$^{-/-}$ or Id3$^{-/-}$ mice.[17,18]

[1]Department of Infectious Diseases and Clinical Microbiology, Beijing Chao-Yang Hospital, Beijing Institute of Respiratory Medicine, Capital Medical University, Beijing, China; [2]Department of Immunology, School of Basic Medical Sciences, Capital Medical University, Beijing, China; [3]Institute of Laboratory Animal Sciences, Chinese Academy of Medical Sciences, Beijing, China; [4]National Institute for Viral Disease Control and Prevention, Chinese Center for Disease Control and Prevention (China CDC), Beijing, China; [5]Department of Respiratory Medicine, Capital Medical University, Beijing, China; [6]Beijing Institute of Respiratory Medicine, Beijing Key Laboratory of Respiratory and Pulmonary Circulation Disorders, Beijing, China and [7]Beijing Institute of Respiratory Medicine, Beijing Hospital, Ministry of Heath, P. R. China, Beijing, China

*Corresponding author: B Cao, Department of Infectious Diseases and Clinical Microbiology, Beijing Chao-Yang Hospital, Beijing Institute of Respiratory Medicine, Capital Medical University, No.8, Gongti South Road, Chaoyang District, Beijing 100020, China. Tel: +86 10 85231167; Fax: +86 10 85231514; E-mail: caobin_ben@yahoo.com

or C Wang, Department of Respiratory Medicine, Capital Medical University; Beijing Institute of Respiratory Medicine, Beijing Key Laboratory of Respiratory and Pulmonary Circulation Disorders; Beijing Institute of Respiratory Medicine, Beijing Hospital, Ministry of Heath, P. R. China, Beijing 100730, China. Tel: +86 10 68792233; Fax: +86 10 68792233; E-mail: cyh-birm@263.com

or C Qin, Institute of Laboratory Animal Sciences, Chinese Academy of Medical Sciences, No.5, Pan Jia Yuan Nan Li, Beijing 100021, China. Tel: +86 10 67770815; Fax: +86 10 67710812; E-mail: qinchuan@pumc.edu.cn

[8]These authors contributed equally to this work.

Abbreviations: HPAIV, highly pathogenic avian influenza virus; NK, natural killer; $TCID_{50}$, 50% tissue culture infective dose; dpi, days post infection; n.i., non-infection; DP, double positive; SP, single positive; MLN, mediastinal lymph nodes; TNF, tumor necrosis factor; IL, interleukin; Eomes, Eomesodermin; Treg, regulatory T cell

Received 03.3.14; revised 02.7.14; accepted 02.7.14; Edited by H-U Simon

Subsequently, it was found that ~10% of TCR$\alpha\beta^+$ CD4$^-$ CD8$^+$ thymocytes were innate polyclonal T cells (CD8$^+$ CD44^{hi}) in normal mice.[19] Whether innate CD8$^+$ thymocytes are involved in the pathogenesis of influenza A(H1N1)pdm09-induced thymic atrophy should be further evaluated.

In this study, we demonstrated that severe influenza A(H1N1)pdm09 infection induced strong thymic atrophy. The viruses could infect the thymus, and further primed the innate CD8$^+$CD44^{hi} T cells. Innate CD8$^+$ T cells induced apoptosis of thymocytes by upregulating IFN-γ. Our results indicated that the pathogenesis of influenza A(H1N1)pdm09 infection was not only due to severe lung damage but also due to innate CD8$^+$ T-cell-induced thymic atrophy.

Results

Severe influenza H1N1 virus infection induced thymic atrophy. BALB/c mice were infected with A/California/07/2009 at 10^6 $TCID_{50}$ to assess whether severe influenza A(H1N1)pdm09 infection could also induce thymic atrophy. At 7 days post infection (dpi), the mice lost ~35% of their weight and had a 20% survival rate. Strikingly, severe thymic atrophy was demonstrable in severely infected mice (Figure 1). At 2 dpi, thymus began to atrophy slightly, and then it showed significant atrophy and drastically reduced size at 5 dpi (Figure 1a). As shown in Figure 1b, the thymic weights of infected mice were significantly reduced at 2 dpi, with 24.6, 73.8, 83.4 and 81.5% weight loss at 2, 3, 5 and 7 dpi, respectively. The number of thymocytes also acutely decreased, leading to 33.8, 83.4, 94.4 and 95.7% reduction at 2, 3, 5 and 7 dpi, respectively (Figure 1c). This decrease in thymocyte number paralleled with the dramatic reduction in thymic weights. Hematoxylin & eosin (H&E) staining showed that the atrophy mainly occurred in the cortex of thymus. Thymocytes filled the cortical areas, and a thick zone of densely stained cortex and a narrow zone of lightly stained medulla were observed in non-infected (n.i.) thymus. However, a substantial reduction in the thickness of cortex and depletion in cortical thymocytes began at 2 dpi; this depletion gradually worsened until the thymocytes were nearly absent at 7 dpi (Figure 1d). Furthermore, flow cytometry analysis showed that the ratios of thymocyte subsets also underwent a dramatic decrease in CD4$^+$CD8$^+$ double-positive (DP) thymocytes and an increase in CD4$^+$ single-positive (SP) and CD8$^+$ SP populations (Figure 1e). DP thymocytes constituted 60–80% of the thymocytes in control mice but were nearly absent (<5%) after virus infection at 5 dpi (Figure 1e). Cell counts of all subgroups showed that all cells, including the double negative (DN), SP and DP T cells, which were reduced with DP thymocytes were the most significantly

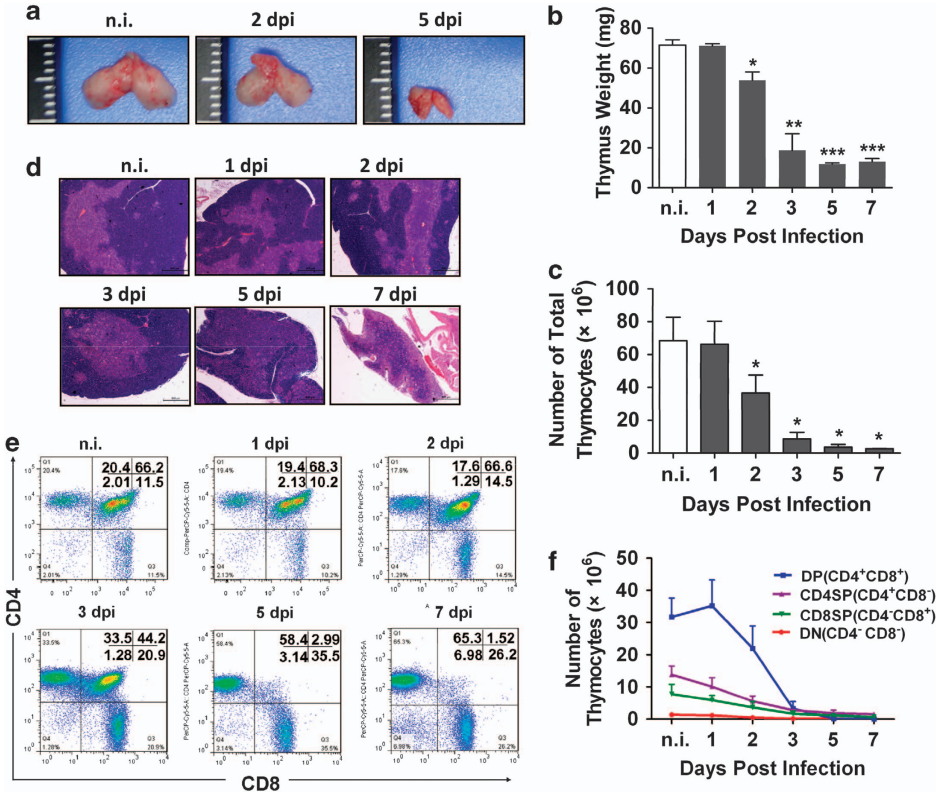

Figure 1 Thymic atrophy induced by severe influenza A(H1N1)pdm09 infection. (**a**) Morphology of a control (n.i.) and influenza virus-infected (2 dpi and 5 dpi) thymus in mice. (**b**) Changes in weight and (**c**) the number of total thymocytes in non-infected or 1, 2, 3, 5 or 7 dpi thymuses ($n=3$). (**d**) H&E staining showing thymus histology in response to H1N1 influenza A virus infection at different dpi (original magnification, ×50). (**e**) Changes in the ratios of different thymocyte subsets (DN, SP and DP) analyzed by flow cytometry in non-infected or 1, 2, 3, 5 or 7-dpi thymuses ($n=3$). FACS plots were gated on thymocytes. One representative FACS plot is presented, and the percentages indicate the proportions of DN, CD8$^+$SP, CD4$^+$SP and DP cells. (**f**) Changes in the number of DN, SP and DP thymocytes from non-infected or 1, 2, 3, 5 or 7 dpi thymuses ($n=3$). The data are presented as the mean ± S.D. ($n=3$). The histogram represents the mean of three independent experiments. Significant differences from the non-infected control were revealed by an unpaired, two-tailed *t*-test. $^*P<0.05$, $^{**}P<0.01$ and $^{***}P<0.001$

depleted ones (Figure 1f). These results suggested that influenza A(H1N1)pdm09 infection induced thymic atrophy, especially of the cortex, and this was accompanied by the dramatic depletion of cortical DP T cells.

Apoptosis was the main reason for DP thymocytes depletion. The DP subsets in the mediastinal lymph nodes (MLN), spleen, peripheral blood and lungs were analyzed by flow cytometry to determine whether virus could induce the premature escape of DP thymocytes. No significant increase in the DP subsets was found in the peripheral organs (Figure 2a), suggesting that the premature escape of DP thymocytes was not the main reason for thymic atrophy. Furthermore, thymocyte apoptosis was detected. As shown in Figure 2b, the thymus of infected mice showed a significantly higher percentage of apoptosis when compared with n.i. mouse at 2 and 3 dpi (~7 and 3.5 *versus* 1.5 apoptotic cells per 10^4 μm^2; Figure 2c), and apoptotic cells in infected thymus were predominantly distributed in the cortical zones. This result was consistent with the dramatic loss of DP cells, which were mainly distributed in the cortical zones. The percentage of apoptotic cells was calculated based on annexin-V and propidium iodide (PI) staining. The percent of annexin-V$^+$ cells was ~40% at 2 dpi, compared with only 14% in control (Figure 2d). Further analysis showed that most of the apoptotic cells (annexin-V$^+$) were DP T cells (Figure 2e), which were consistent with thymic cortex atrophy and the dramatic depletion of DP T cells. Taken together, these results suggested that apoptosis, but not escape, was the main reason for thymic atrophy and DP thymocyte depletion.

Influenza A(H1N1)pdm09 viruses were present in DCs of thymus. To further analyze whether influenza A(H1N1)pdm09 virus were present in thymus of severely infected mice, immunohistochemistry was performed. The results showed

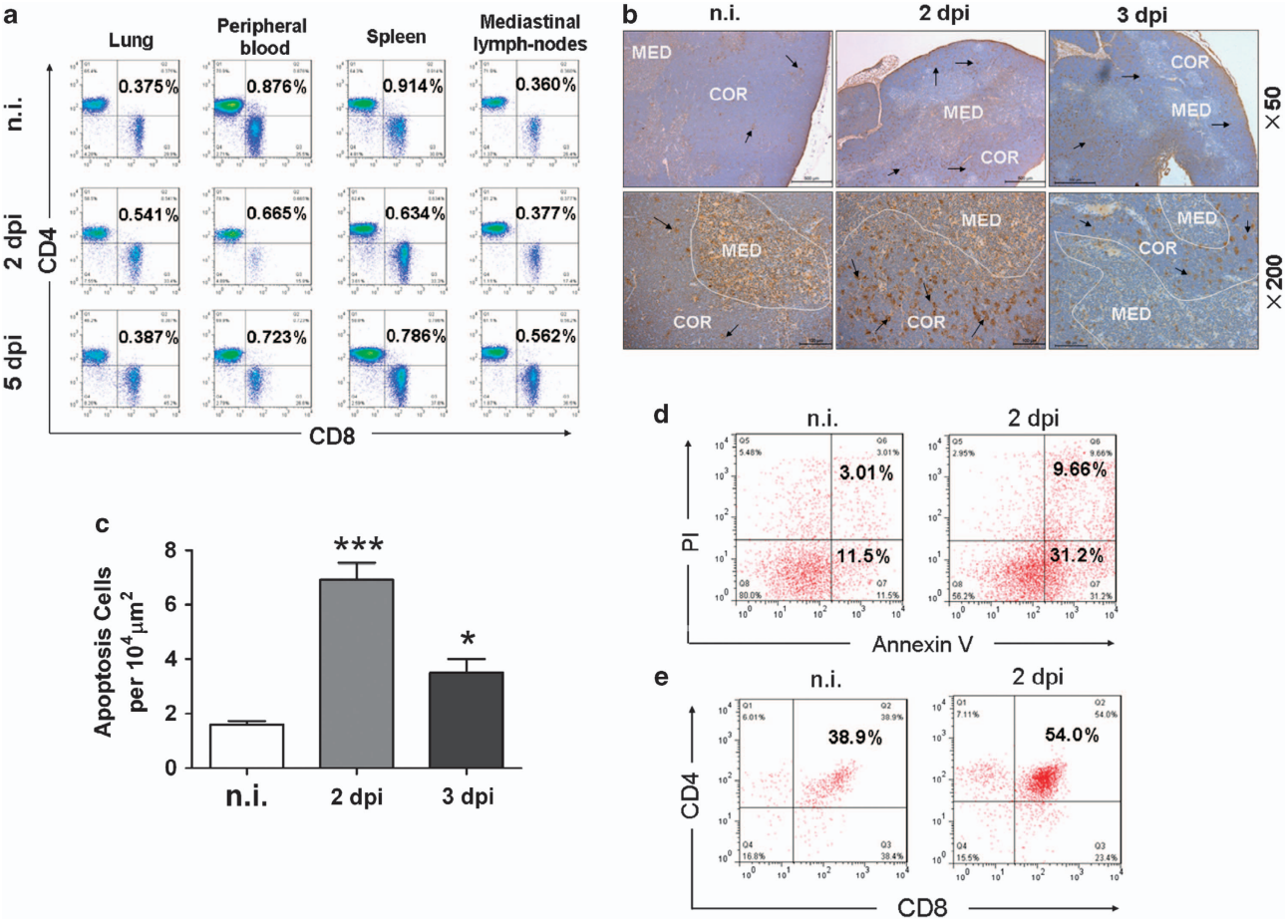

Figure 2 Detection of the DP subset in peripheral organs and apoptosis of thymocytes in the thymus. (**a**) DP subsets in the mediastinal lymph nodes (MLN), spleen, peripheral blood and lungs of control or 2-dpi and 5-dpi mice were analyzed by flow cytometry; the FACS plots were gated on CD3$^+$ lymphocytes. Percentages indicate the proportions of CD4$^+$CD8$^+$ DP cells. (**b**) *In situ* detection of thymocyte apoptosis using the *In Situ* Cell Death Detection Kit (TUNEL assay). The brown stain represents DNA fragmentation of apoptotic cells, and the blue stain shows the nuclei stained with hematoxylin. There were more apoptotic cells in the COR at 2 and 3 dpi compared with the non-infected thymus. Arrows indicate positive staining. (**c**) Apoptotic cells per 10^4 μm^2 were counted in the cortex. (**d**) The apoptotic thymocytes were identified by annexin-V and PI staining. The FACS plots were gated on thymocytes. One representative FACS plot is presented, and the percentages indicate the proportions of apoptotic cells. (**e**) The annexin-V-positive thymocytes were identified by CD4 and CD8 staining. The percentages indicate the proportions of CD4$^+$CD8$^+$ DP cells. The data are presented as the mean ± S.D. ($n = 3$). Significant differences from the non-infected control were determined by an unpaired two-tailed *t*-test. *$P < 0.05$, ***$P < 0.001$. COR, cortex; MED, medulla

that large amounts of influenza A(H1N1)pdm09 virus were present in lung epithelial cells. Strikingly, virus were also present in the thymus, especially in the cortical region, at 2 dpi (Figure 3a). Further qRT-PCR and influenza virus titration assay identified the presence of virus in the thymus at 2, 3 and 5 dpi (Figures 3b and c). The location was further confirmed using confocal immunofluorescence. As shown in Figure 3d, some of the influenza A(H1N1) pdm09 virus were present within DCs. These results demonstrated that influenza A(H1N1) pdm09 virus could be translocated to thymus, and might prime and activate immune response.

Elevated IFN-γ and other proinflammatory cytokines in the thymus. Influenza A(H1N1)pdm09 caused hypercytokinemia in the lungs and serum.[20] However, changes in the thymus were not determined. To evaluate the changes of secreting cytokines and chemokines, the Bio-plex system was used to analyze the levels of certain cytokines and chemokines in thymus. Compared with control mice, infected mice exhibited significant elevation of proinflammatory cytokines and chemokines, such as interleukin-1α/β (IL-1α/β), IL-6, IL-12 (p70), IL-17, IL-17F, IFN-γ, tumor necrosis factor-α (TNF-α), G-CSF, MCP-1 and RANTES (Figures 4a–g and Supplementary Figure 1). Increased levels of GCs are widely recognized as a common cause for increased thymocyte apoptosis and lymphopenia during severe infection.[21,22] However, the levels of serum corticosterone were not elevated in our infection model, suggesting that endogenous GCs was not involved in influenza A(H1N1)pdm09-induced thymic atrophy (Figure 4i). IL-7 is a cytokine that is essential for T-cell survival in thymus.[23,24] As shown in Supplementary Figure 1, the transcription of IL-7 mRNA was not decreased but rather increased in the thymus after

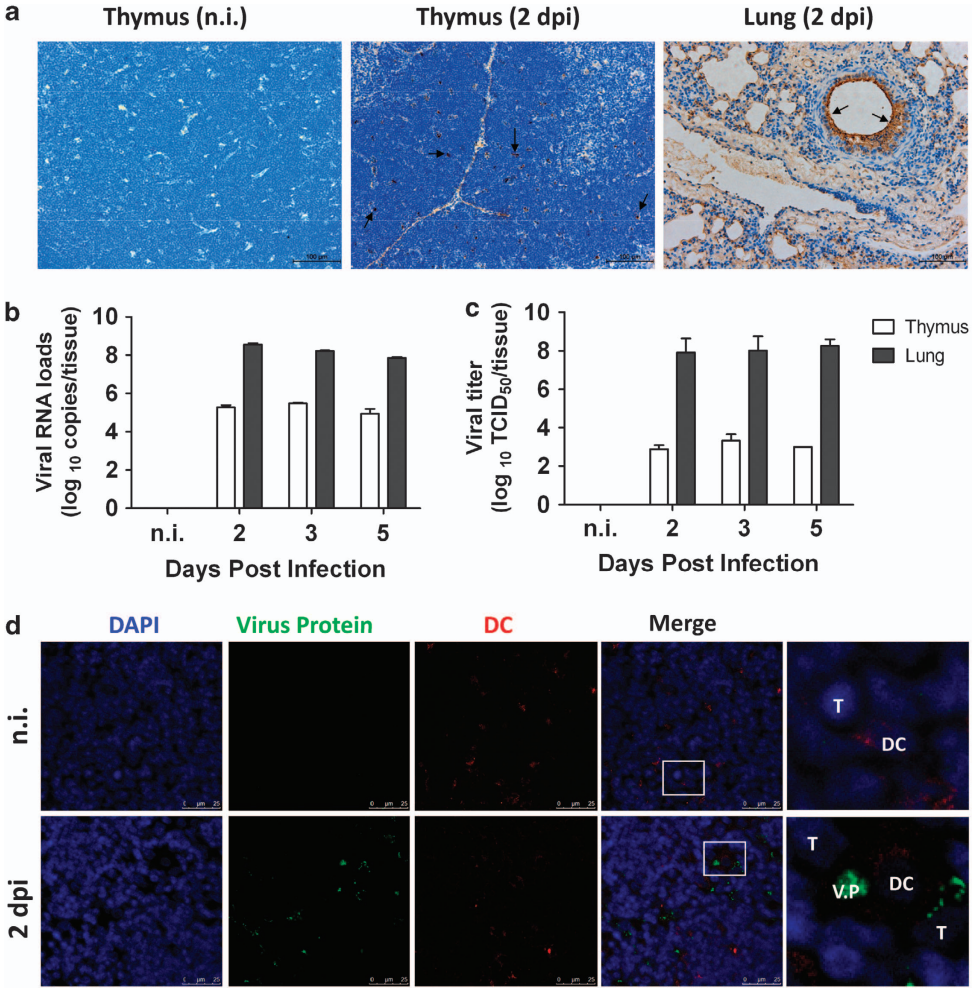

Figure 3 Presence of influenza A(H1N1)pdm09 virus in the thymus. (**a**) Influenza A virus-encoded protein was detected using immunohistochemistry with the anti-influenza A virus antibody. Virus-encoded protein was present in the thymus of 2-dpi mice, but not in non-infected mice. Lung tissue from 2-dpi mice was used as the positive control. The brown stain represents the virus protein-positive cells, and the blue stain shows nuclei stained with hematoxylin. Arrows indicate positive staining (original magnification, $\times$ 200). (**b**) The virus HA gene was detected in the thymus and lungs of non-infected or infected mice at 2, 3 and 5 dpi by qRT-PCR ($n = 6$). The values were shown as mean $\pm$ S.D. (**c**) Growth properties of viruses. At 2, 3 and 5 dpi, thymus and lung tissues were collected, and virus titers were determined by plaque assays in MadinDarby canine kidney cells. The values were presented as mean $\pm$ S.D. from six mice. (**d**) Confocal immunofluorescence analysis of virus-encoded proteins and DCs. Virus-encoded protein labeled with anti-influenza A virus antibody was shown in green, DCs labeled with the rat anti-mouse dendritic/interdigitating cell antibody were shown in red, and nuclei stained by DAPI were shown in blue (original magnification, $\times$ 630). DC, dendritic cell; T, thymocytes; VP, virus-encoded protein

infection, suggesting that IL-7 was also not involved in thymic atrophy. Given the important role of IFN-γ in immunomodulatory and inducing apoptosis, we further evaluated the transcription of IFN-γ using qRT-PCR. As shown in Figure 4h, IFN-γ transcription was increased in a time-dependent manner, with approximate fold increases of 1.4, 8.3 and 50.1 at 1, 2 and 5 dpi, respectively. The rapid and significant increase in IFN-γ, even at 1 dpi, corresponded to aggravated thymic atrophy, which demonstrated the pivotal roles of innate immune cells, such as innate CD8$^+$ thymocytes, natural killer (NK), $\gamma\delta$T cells and macrophages in thymus.

Thymic innate CD8$^+$ T cells were activated and secreted IFN-γ. Due to the presence of influenza A(H1N1)pdm09 virus and increased IFN-γ in thymus, we investigated which cells were activated and secreted IFN-γ after infection. We first detected whether the conventional CD8$^+$ T lymphocytes in the thymus were activated by influenza virus presented by DCs. A tetramer assay was performed using H-2Kd loaded with TYQRTRALV, which was derived from the viral nucleoprotein $(NP)_{147-155}$.[25] We found the ratio of NP-specific CD8$^+$ T cells increased from 0.08% in uninfected lung to 3.41% and 9.69% in infected lung at 2 dpi and 5 dpi, respectively (Supplementary Figure 2A). However, NP-specific CD8$^+$ T cells were nearly absent and had no obvious increase in thymus after infection (Supplementary Figure 2A), and the ratio of NP-specific CD8$^+$ T cells were only 0.11% and 0.35% in infected mice at 2 dpi and 5 dpi, respectively (Supplementary Figure 2A). Perforin and granzyme B were another mechanism for CD8$^+$ T-cell-mediated cytotoxicity. It was found that influenza A(H1N1)pdm09 did not induce the expression of perforin or granzyme B on CD8$^+$ SP cells (Supplementary Figures 2B and C). These results demonstrated that functional, virus-specific conventional CD8$^+$ T lymphocytes had no roles in the influenza A(H1N1)pdm09-induced thymic atrophy. Due to the significant raise of IFN-γ as shown in Figures 4g and h, we then search the resource of IFN-γ. As shown in Figure 5a, the percent of IFN-γ^+ cells were increased from 1.8% in control thymus to 3.5% and 3.4% in 2 dpi and 3 dpi thymus, respectively. Thymic CD8$^+$, CD4$^+$ T cells, NKT and $\gamma\delta$T cells can secrete IFN-γ after infection. It was demonstrated that CD4 SP T cells and DP T cells could only secrete a little amount of IFN-γ and had no obvious increase after virus infection (Supplementary Figures 3A and B); furthermore, the percent of NKT and $\gamma\delta$T cells degressed after infection, and among the IFN-γ^+ cells, NKT and $\gamma\delta$T cells were only 3.4% and 2.1%, respectively (Supplementary Figures 4A and B). The results suggested that CD4 SP T cells, DP T cells, NKT and $\gamma\delta$T cells were not the main resource of IFN-γ. Surprisingly, the ratio of IFN-γ^+ cells was about 3% of the CD8 SP T subset in uninfected thymus; however, the ratio of IFN-γ^+ cells increased to 12% and 9.5% of CD8 SP T cells in infected thymus at 2 dpi and 3 dpi, respectively (Figure 5b). Further analysis showed that more than 85% of IFN-γ^+ cells were CD8 SP T cells, and also they can exhibit high expression of CD44 (Figure 5c). As showed in Figure 5d, almost all the IFN-γ^+ cells were CD44^{hi} among CD8 SP T cells, and the percent of CD8$^+$CD44^{hi}IFN-γ^+ cells raised from 4.4% in control thymus to 9% in infected thymus at 2 dpi and 3 dpi, respectively. Further analysis showed that the

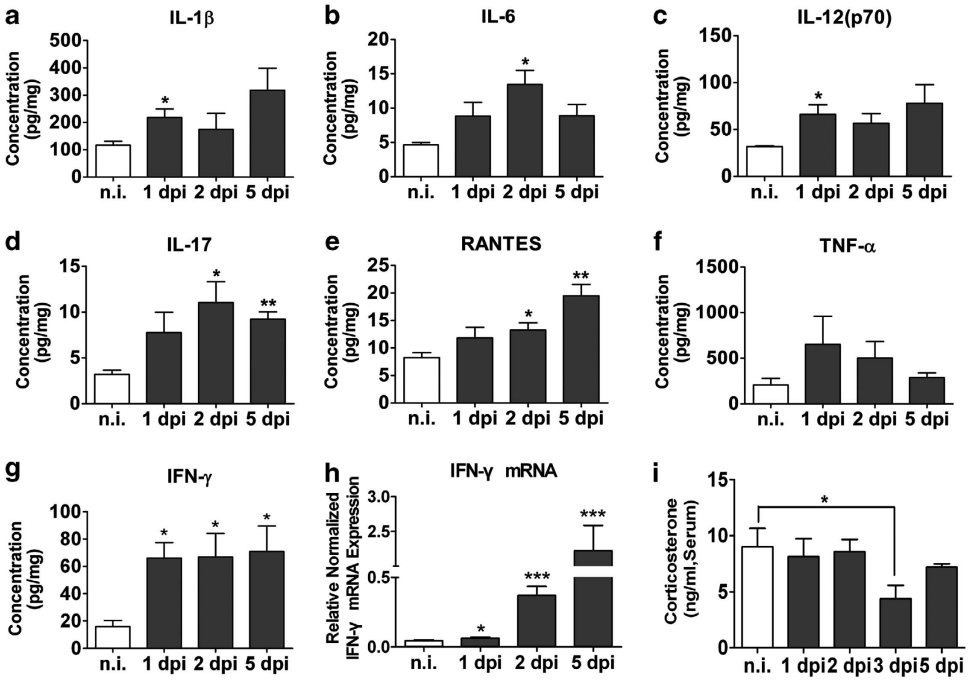

Figure 4 Assessment of cytokine levels in the thymus and concentration of corticosterone in the serum. (**a–g**) The concentrations of certain associated cytokines in the thymus were determined using the Bio-Plex Mouse Cytokines 23-Plex panel and Th17 8-Plex panel arrays and normalized to homogenized thymus protein content. (**h**) Elevated IFN-γ mRNA transcription analyzed by quantitative real-time PCR. (**i**) Concentration of corticosterone in the serum was measured by ELISA. The data are presented as the mean ± S.D. ($n = 3$). Significant differences from the non-infected control were revealed by an unpaired two-tailed *t*-test. $^*P < 0.05$, $^{**}P < 0.01$ and $^{***}P < 0.001$

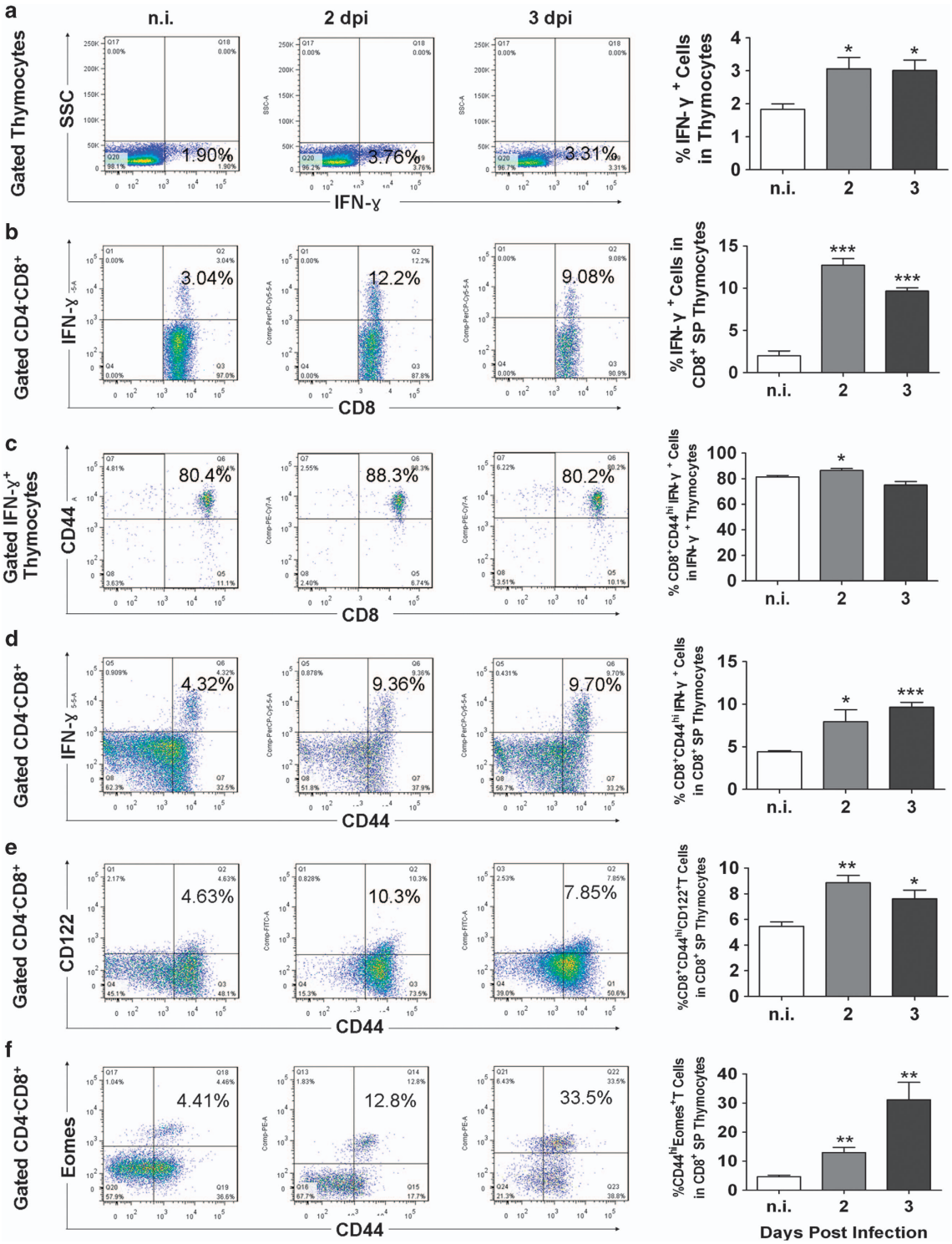

Figure 5 Increased percentage of innate CD8$^+$CD44^{hi}CD122$^+$Eomes$^+$ SP T cells in the thymus of infected mice. (**a**) Increased percentage of IFN-γ^+ cells in the thymocytes after infection at 2 and 3 dpi. (**b**) Increased percentage of IFN-γ^+ cells in the CD8$^+$ SP T cells, as determined by flow cytometry. The FACS plots were gated on CD8$^+$ SP thymocytes. Percentages indicated the proportions of IFN-γ^+ cells. (**c**) Most of the cells were CD8$^+$CD44^{hi} among the IFN-γ^+ thymocytes. Percentages indicated the proportions of CD8$^+$CD44^{hi} cells in IFN-γ^+ thymocytes. (**d**) All the CD8$^+$IFN-γ^+ cells highly expressed CD44. Percentages indicated proportions of IFN-γ^+CD44^{hi} in CD8$^+$ SP thymocytes. Analysis of CD44 and CD122 (**e**), and Eomes (**f**) expression on CD8$^+$ SP T cells from non-infected, 2-dpi or 3-dpi thymuses. One representative FACS plot is presented. Values represent the means ± S.D. ($n = 6$) of three independent experiments. Significant differences from the non-infected control were revealed by an unpaired two-tailed *t*-test. *$P < 0.05$, **$P < 0.01$ and ***$P < 0.001$

percent of CD8$^+$CD44^{hi}CD122$^+$ cells raised from 5.1% in control thymus to 9.8% and 8% in infected thymus at 2 dpi and 3 dpi, respectively, (Figure 5e), and 35% of CD8$^+$CD44^{hi}CD122$^+$ (but only 3.3% of CD8$^+$CD44^{low}CD122$^-$) cells could secrete IFN-γ (Supplementary Figure 5). In addition to conventional CD8$^+$ T cells, innate T cells, which are defined as CD8$^+$CD44^{hi}CD122$^+$, were also found in normal thymus.[18,19] They served as an initial control for infection through swiftly initiating proliferation and rapidly secreting proinflammatory cytokines, such as IFN-γ and TNF-α.[16–19] The level and TNF-α was also immediately increased, even at 1 dpi (Figure 4f). In addition, IL-2 and IL-4, which are essential for innate T-cell expansion and development, were expressed during the infection process (Supplementary Figure 1). Eomesodermin (Eomes) was the most important and essential transcription factor for the development and function of innate T cells.[19,26] As showed in Figure 5f, the ratio of CD44^{hi}Eomes$^+$ thymocytes raised from 4.5% in control thymus to 13% and 35% in infected thymus among CD8 SP T cells at 2 dpi and 3 dpi, respectively. Furthermore, almost all the CD8$^+$CD44^{hi}IFN-γ^+ thymocytes were Eomes$^+$ (Supplementary Figure 6A), and reversely, about 50% of CD8$^+$CD44^{hi}Eomes$^+$ thymocytes secreted IFN-γ (Supplementary Figure 6B). Elevated IFN-γ expression on CD8$^+$CD44^{hi}CD122$^+$Eomes$^+$ cells suggested the activation of thymic innate T cells. These results demonstrated that thymic innate T cells could be activated by influenza A(H1N1)pdm09 virus and might mediate thymic atrophy through secreting IFN-γ.

Milder thymic atrophy was observed in C57BL/6J mice. Whether low number of thymic innate CD8$^+$ T cells could mitigate influenza A(H1N1)pdm09-induced thymic atrophy was then investigated. It was found that more innate CD8$^+$ T cells were present in BALB/c strain thymus than in C57BL/6J strain thymus.[18,19] As shown in Figures 6a and b, only $<1\%$ of CD8$^+$ T cells were innate T cells in C57BL/6J strain thymus ($>4\%$ in BALB/c strain as shown in Figure 5d). The ratio of IFN-γ^+ cells was $<1\%$ of CD8 SP T subset in uninfected C57BL/6J mice thymus; and the IFN-γ^+ thymocytes increased nearly 2% of CD8 SP T cells at 2 dpi and then decreased to 1% at 3 dpi (Figure 6a); and the percent of CD8$^+$CD44^{hi}IFN-γ^+ cells raised only from 0.8% in control thymus to 1.6% in infected thymus at 2 dpi and then immediately decreased to 0.8% at 3 dpi (Figure 6b), which was far less than that observed in BALB/c mice (9% as showed in Figure 5d). Meanwhile, thymic atrophy of C57BL/6J mice was milder than that of BALB/c mice (Figure 6c), which suggested that low percent of innate T cells could relieve influenza A(H1N1)pdm09-induced thymic atrophy.

Peramivir did not significantly alleviate thymic atrophy. We next investigated whether antiviral agents could suppress thymic atrophy. As shown in Figure 7a, peramivir had only a little protective role on thymic weight decrease at 2 and 5 dpi, but peramivir could significantly protect lung injury. Viral loads of 2 and 5-dpi-infected thymuses also had only minor decreasion after peramivir treatment (Figure 7b). The ratio of IFN-γ^+ cells increased from 3% of CD8 SP T subset

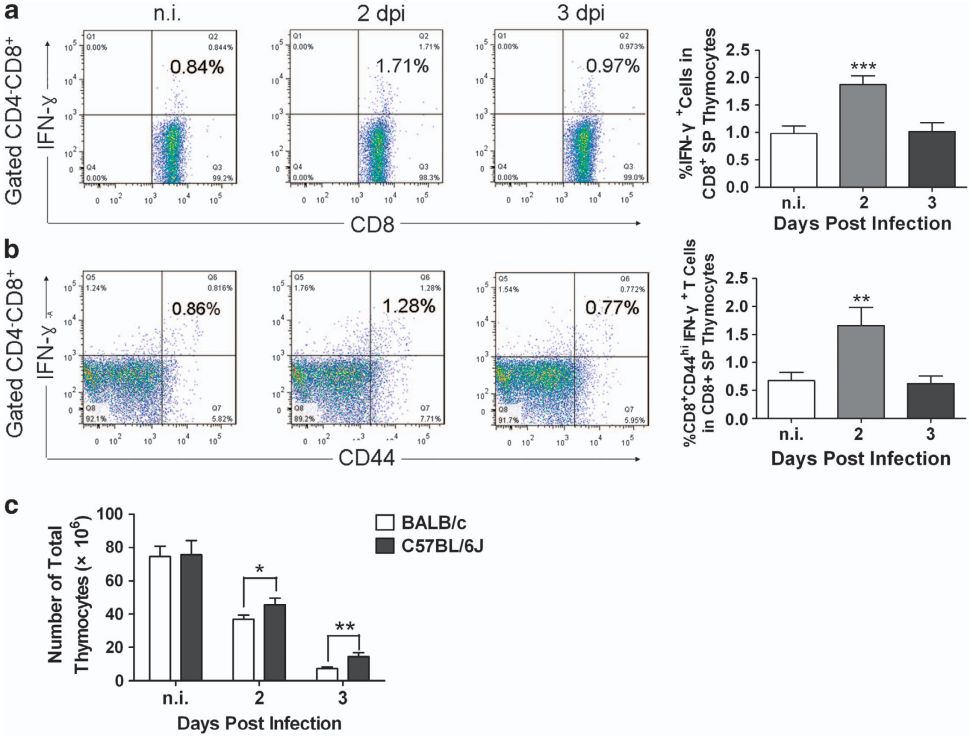

Figure 6 Milder thymic atrophy and lower innate CD8$^+$CD44^{hi} T cells in the thymus of C57BL/6J mice. C57BL/6J and BALB/c mice were intranasally infected with influenza A virus strain A/California/07/2009 at 10^6 $TCID_{50}$, (**a**) Percentage of IFN-γ^+ cells, (**b**) innate CD8$^+$CD44^{hi} T cells among CD8$^+$ SP T-cell population in non-infection, 2- and 3-dpi-infected C57BL/6J mice, as determined by flow cytometry. The FACS plots were gated on CD8$^+$ SP thymocytes. Percentages indicate the proportions of IFN-γ^+ cells. (**c**) The numbers of total thymocytes in non-infected or 2-, 3-dpi thymuses were evaluated. The data are presented as the mean ± S.D. ($n=5$). Significant differences compared with the non-infected control are shown. *$P<0.05$, **$P<0.01$ and ***$P<0.001$

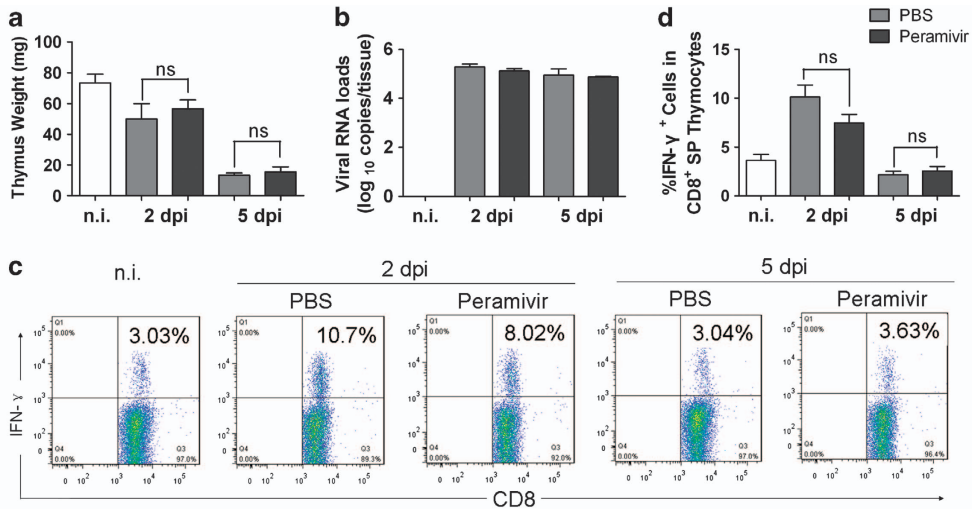

Figure 7 Peramivir did not significantly improve the thymic atrophy induced by severe influenza A(H1N1)pdm09 infection. Mice were treated intraperitoneally with PBS or peramivir at a dose of 40 mg/kg daily for 5 days. (**a**) Changes in thymus weight of non-infected, influenza virus-infected and peramivir-treated mice, or influenza virus-infected and PBS-treated mice. (**b**) Viral RNA loads of peramivir or PBS-treated mice thymus at 2 and 5 dpi. (**c**,**d**) Percentage of IFN-γ^+ cells in the CD8$^+$ SP T-cell population from thymus of non-infected, influenza virus-infected and peramivir- or PBS-treated mice on 2 and 5 dpi ($n = 6$). One representative FACS plot is presented. Values represent the mean ± S.D. Significant differences from the non-infected control were revealed by an unpaired two-tailed *t*-test. ns, not significant

in uninfected thymus to 10% at 2 dpi; however, peramivir treatment didn't significantly decrease the ratio of innate CD8$^+$IFN-γ^+ thymocytes (Figures 7c and d). The results demonstrated that inhibition of thymic innate CD8$^+$ T cells, but not using antiviral drugs, could rescue the influenza A(H1N1)pdm09 virus-induced thymic atrophy.

IFN-γ has a critical role in the thymic atrophy. Thymic innate CD8$^+$ T cells mediated thymic atrophy through IFN-γ secretion. Whether neutralization of IFN-γ could suppress the thymic atrophy was then investigated. As shown in Figure 8a, neutralization of IFN-γ could significantly suppress the atrophy, the thymus size of IFN-γ neutralization group was obviously larger than the PBS control group. The thymus weight was significantly decreased to 25% and 10% at 3 dpi and 5 dpi, respectively, and IFN-γ neutralization antibody significantly rescued the decrease and with only 50% weight loss; the thymus weight of IFN-γ neutralization antibody treatment mice were two folds of that of the PBS control mice at 3 and 5 dpi (Figure 8b). Meanwhile, IFN-γ neutralization antibody treatment significantly decreased the apoptosis of thymocytes from 15% in control thymus to 10% at 5 dpi (Figure 8c). Furthermore, flow cytometry analysis showed that IFN-γ neutralization antibody treatment dramatically rescued the decrease of DP thymocytes; the DP thymocytes constituted 70% of the thymocytes in control mice, and it was decreased to 40% and 3% at 3 dpi and 5 dpi, respectively, however, it was only decreased to 55% and 10% at 3 dpi and 5 dpi, respectively, by neutralizing IFN-γ (Figure 8d). The percent of CD8$^+$CD44^{hi}CD122$^+$ innate T cells were only increased to 6.7% and 2.5% after IFN-γ neutralization antibody treatment at 3 dpi and 5 dpi, respectively, which was significantly less than that observed in PBS control group (Figure 8e). Furthermore, the percent of Eomes (essential transcription factor for the development and function of innate T cells[19,26]) positive innate T cells were significantly less in IFN-γ neutralization antibody treatment group than that in PBS control group at 3 and 5 dpi (Figure 8f). The results suggested that IFN-γ has a critical role to play during the influenza A(H1N1)pdm09-induced thymic atrophy.

Discussion

The thymus is a primary lymphoid organ where T-cell development takes place, and it has an important role in protecting against pathogen infection. However, several pathogens can cause thymic atrophy, including viruses, parasites and fungi.[11,13,27–33] Thymic atrophy may further interfere with the systemic cellular immune response and delay the clearance of pathogen. Common histological features that can be observed during different infections include a decrease in cortical thymocytes and a loss of the clear-cut distinction in corticomedullary region.[11,27,32,34] Because the mechanisms involved in infection-induced thymic atrophy are not completely understood and may vary depending on the microorganism, the determination of specific pathways in distinct situations is essential to define strategies for preventing thymic atrophy and/or promoting the recovery of thymic function once the infection is controlled. Here, we showed that severe influenza A(H1N1)pdm09 infection induced thymic atrophy via the activation of innate CD8 thymocytes in BALB/c mouse model.

Thymic atrophy in infectious disease may result from the following four events: (1) a decreased number of precursor cells entering into the thymus, (2) lower capacity for thymocyte proliferation, (3) increased thymocyte apoptosis/death and (4) increased exit of thymocytes to peripheral lymphoid tissues. Previous reports demonstrated that influenza virus was not present in bone marrow and did not influence precursor cell entry into the thymus.[13] In current study, an acute decrease of thymocytes was induced at 2 dpi, and were nearly absent at

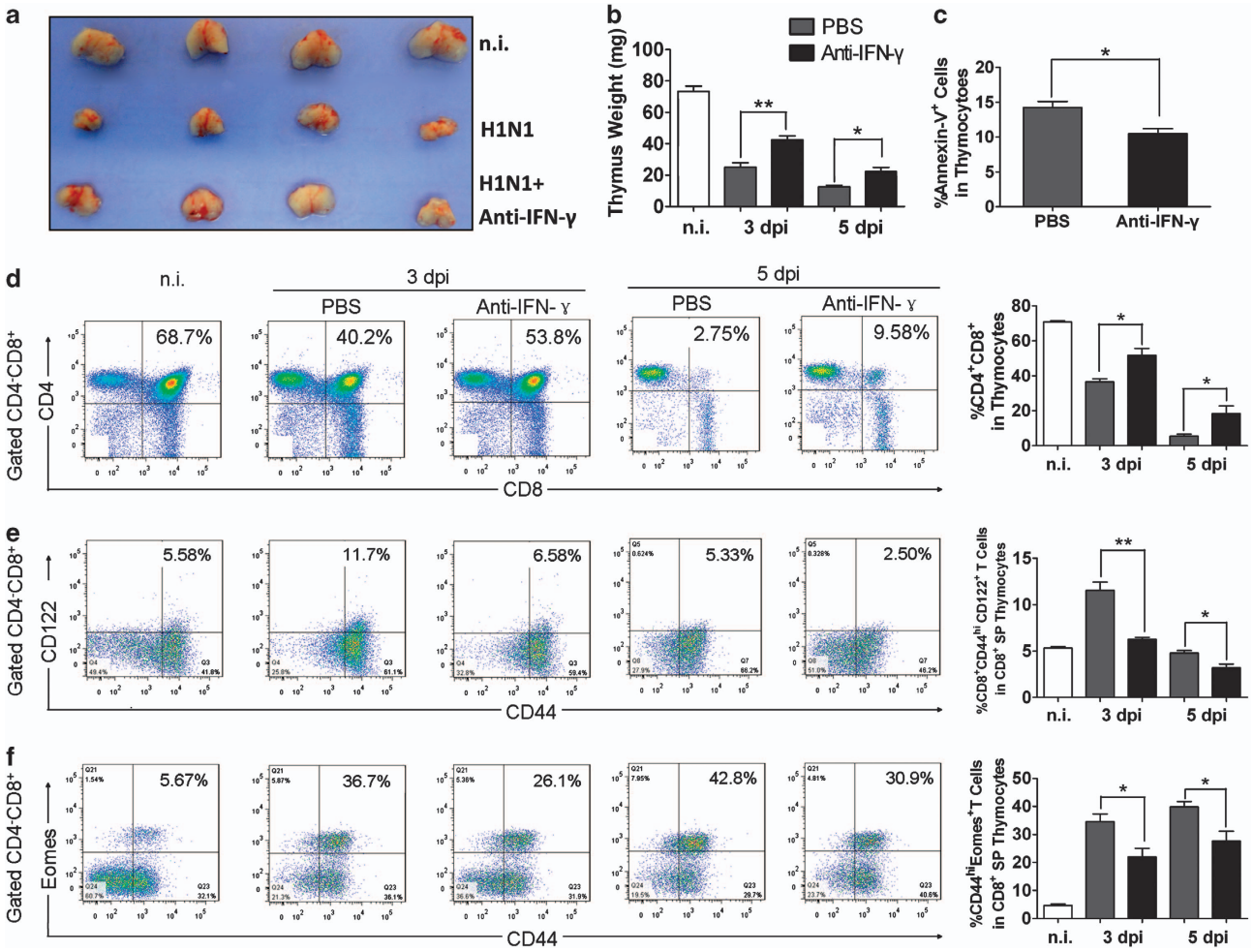

Figure 8 Neutralization of IFN-γ-ameliorated influenza A(H1N1)pdm09-induced thymic atrophy. For neutralizing endogenous IFN-γ, mice were either intraperitoneally injected with the rat anti-mouse IFN-γ monoclonal antibody or with PBS as control. (**a**) Morphology of a non-infected, influenza virus-infected and anti-IFN-γ or PBS-treated thymus at 3 dpi. (**b**) Changes in thymus weight of non-infected, influenza virus-infected (3 dpi and 5 dpi) and anti-IFN-γ or PBS-treated mice ($n=5$). (**c**) The apoptotic thymocytes of anti-IFN-γ or PBS-treated mice at 5 dpi ($n=5$) were analyzed as in Figure 2d. (**d**) Changes in the ratios of the DP thymocytes subset analyzed by flow cytometry in non-infected, influenza virus-infected and anti-IFN-γ or PBS-treated mice ($n=5$). FACS plots were gated on thymocytes. (**e**) Analysis of CD44 and CD122 or (**f**) CD44 and Eomes expression on CD8$^+$ SP T cells ($n=5$). One representative FACS plot is presented. Values represent the means ± S.D. Significant differences from the non-infected control were revealed by an unpaired two-tailed *t*-test. $^*P<0.05$, $^{**}P<0.01$ and $^{***}P<0.001$

7 dpi (Figure 1). These findings excluded the possibility of lower proliferation ability. Premature escape of immature DP T cells from thymus into periphery was one of the main reasons for parasite- and virus-induced thymic atrophy.[32,34] However, no significant increase of DP lymphocytes was observed in the MLN, spleen, peripheral blood or lungs during virus infection (Figure 2a). These results suggested that the premature escape of DP thymocytes was also not the main reason. In fact, influenza A(H1N1)pdm09 infection had already induced a significantly higher percentage of apoptosis (Figures 2b–d). We therefore speculated that the increased apoptosis of thymocytes was one of the main mechanisms in influenza A(H1N1)pdm09-induced thymic atrophy.

The factors that mediate thymocyte apoptosis were further analyzed. Corticosteroids are thought to have a major role in the pathogenesis of *Trypanosoma cruzi*-induced thymocyte death.[30,35,36] However, the level of GCs in serum was not altered (or decreased at 3 dpi) after virus infection, suggesting that the GCs have a minor role (or no role) in our mouse model. The increased production of proinflammatory cytokines had also been proposed to have a role in infection-induced thymic atrophy. For example, *Francisella tularensis*-induced severe thymic atrophy was mediated at least partially by TNF.[37] IFN-α was also a critical molecular mediator of pathogen-induced thymic involution.[38,39] Recently, it was also found that IFN-γ could increase DP thymocyte death during *S. typhimurium*-, *Mycobacterium avium*- or concanavalin A-induced thymic atrophy.[33,38,40] In the current study, elevated expression of proinflammatory cytokines, such as IL-1α/β, IL-6, IL-12, IL-17, IFN-γ and TNF-α, was also noted in influenza A(H1N1)pdm09-infected thymus tissue (Figure 4), suggesting that proinflammatory cytokines may be involved in the thymic atrophy in our model.

DCs are targets for influenza virus infection and can migrate and re-enter into the thymus after uptake of antigens in periphery.[41,42] It was reported that respiratory DCs were able

to transport H5N1 virus from lung into thymus.[13] As shown in Figure 3, influenza A(H1N1)pdm09 could infect thymus and some were present in thymic DCs, suggesting that virus or infected DCs participated in thymic atrophy.

As shown in Figure 4, the levels of proinflammatory cytokines and chemokines were immediately and rapidly increased, even at 1 dpi. Furthermore, the total number of thymocytes was significantly decreased and obvious morphological changes were observed at 2 dpi. We speculated that some thymic innate immune cells might be involved in thymus tissue destruction. Recently, it was reported that innate CD8$^+$ T cells constituted another major population of innate immune cells in thymus.[16,17] These cells can acquire effector function during maturation process in thymus, but does not require activation, proliferation and differentiation. Innate T cells share CD122$^+$CD44^{hi}Eomes$^+$ phenotype and rapidly secrete large amounts of cytokines upon stimulation.[16,17] It was found that $\sim$16% of TCR$\alpha\beta^+$ CD4$^-$CD8$^+$ thymocytes were innate polyclonal T cells in BALB/c mice.[18] In our study, $\sim$13% of CD8$^+$ SP thymocytes were activated (IFN-γ^+) at 2 dpi; it is likely that these cells were innate T cells. On the other hand, most innate T cells are present in cortex region. These findings may explain why cortex and DP thymocytes were depleted to the greatest extent. Interestingly, more innate CD8$^+$ T cells were present in BALB/c strain than in C57BL/6J strain.[18,19] As shown in Figure 6, $<$2% of CD8$^+$ SP thymocytes were IFN-γ^+ at 2 dpi in C57BL/6J mice, which was far less than that observed in BALB/c mice. This corresponded to a milder thymic atrophy in C57BL/6J mice. But how virus activated innate T cells should be further studied. In contrast to our results, Vogel *et al.*[13] reported that A/Regensburg/D6/2009 strain did not induce thymic atrophy in C57BL/6J mice. This disparity might be due to differences in the infective dose, strains and mice model. Thymically generated CD4$^+$CD25$^+$Foxp3$^+$ regulatory T cells (Treg) are a cell lineage devoted to the maintenance of homeostasis in the immune system. It is known that acute influenza A virus infection is capable of inducing a robust activation and expansion of suppressive Treg response, which are critical for suppressing excessive immunopathological responses to pathogens through the secretion of large amounts of IL-10.[43–45] We found that the percent of CD4$^+$Foxp3$^+$ Treg among CD4 SP thymocytes was significantly elevated, more than twofolds, compared with n.i. control at 3 dpi (Supplementary Figure 7). As shown in Supplementary Figure 1, the concentration of IL-10 in thymus was increased after infection, which suggested the activation of Treg. Otherwise, the percentage of IFN-γ^+ cells was gradually degraded at 3 and 5 dpi compared with 2 dpi (Figures 5b and 7c), which suggested Treg might influence the IFN-γ secretion of innate CD8$^+$ T cells. Additional experiments should be performed for the sake of confirmation.

The existence of activated innate CD8$^+$ T cells in thymus is crucial and might lead to organ destruction via secretion of large amounts of IFN-γ upon stimulation.[16,17,19] Neutralization of IFN-γ could significantly rescue the atrophy and the depletion of DP thymocytes (Figure 8), but peramivir treatment did not significantly alleviate thymic atrophy (Figure 7). Additional experiments should be performed to explain the mechanism of IFN-γ in pathology. Our current understanding of the complex picture underlying thymic atrophy during influenza A(H1N1)pdm09 infection is limited, and cross-talk between different pathways may occur.[40]

Collectively, during the course of infection, influenza A(H1N1)pdm09 can be translocated to thymus via DCs, and subsequently activate innate CD8$^+$ T cells to swiftly initiate proliferation and secrete high quantities of IFN-γ, which mediates thymocyte apoptosis and thymic atrophy. Innate CD8$^+$ T cells were able to initially control virus infection immediately, which served as a first-line defense against virus infection, but they can also cause severe pathological damage. This mechanism may underlie diseases with predominantly increased thymic atrophy in younger people.

Materials and Methods

Mice, virus and infection. Female 4-week-old, specific pathogen-free BALB/c and C57BL/6J mice were obtained from the Institute of Laboratory Animal Sciences (Beijing, China). The influenza A virus strain A/California/07/2009 (H1N1v) was used in this study. Mice were anesthetized and inoculated intranasally with virus (10^6 $TCID_{50}$ in 50 μl) as described in our previous report.[46] Live-mouse experiments and live-virus experiments were performed in Biosafety Level 3 facilities following governmental and institutional guidelines. At the defined time points, the thymus, spleen, lung, MLN and peripheral blood were analyzed as described below. All animal experimental protocols were evaluated and approved by the Institute of Animal Use and Care Committee of the Institute of Laboratory Animal Science, the Peking Union Medical College (ILAS-PL-2012-009).

Virus titrations. The homogenized thymus and lung tissues were collected from six mice on day 2 after inoculation, virus titrations were performed by end-point titration in MadinDarby canine kidney cells, as described previously.[46]

Histological examination and immunohistochemistry analysis. Thymuses were fixed in 10% neutral-buffer formalin for 24 h and subsequently embedded in paraffin. Thymus sections (4–6 μm) from n.i. and 2-dpi mice were deparaffinized and hydrated using xylene and an alcohol gradient. The sections were then stained with H&E for the assessment of general histopathology.

After deparaffinization and hydration of the thymus sections from the n.i. and 2-dpi mice using xylene and gradient alcohol, antigens were retrieved by heating for 15 min in citric acid buffer (1.0 mol/l, pH 6.0) using a microwave and subsequently cooling to room temperature. Different corresponding antibodies were added to each slide and incubated overnight at 4 °C. For influenza A virus-encoded protein detection, anti-influenza A virus antibody (1 : 200 dilution, Abcam, Cambridge, MA, USA) was used. After washing three times with PBS, the Polink-2 plus polymer HRP detection system for goat primary antibody (ZSGB-BIO, Beijing, China) was added. The immune complexes were visualized using 3,3-diaminobenzidine (DAB) Substrate Kit (ZSGB-BIO). The slides were then lightly counterstained with hematoxylin, dehydrated and mounted.

Thymic apoptotic cells were stained by TUNEL using the *In Situ* Cell Death Detection Kit, POD (Roche Applied Science, Mannheim, Germany) according to manufacturer's guidelines. Briefly, sections were fixed in 4% paraformaldehyde, incubated in blocking solution, incubated in permeabilization solution and finally incubated in TUNEL reaction mixture for 60 min at 37 °C. After rinsing, the sections were incubated with Converter-POD for 30 min at 37 °C and developed with the DAB Substrate Kit. The slides were lightly counterstained with hematoxylin, dehydrated and mounted. The slides were photographed using an Olympus AH-2 camera (Olympus, Tokyo, Japan). For each group, four samples were evaluated.

Thymic sections from n.i. and 2-dpi mice were treated as above. Anti-influenza A virus antibody (1 : 200 dilution, Abcam) and rat anti-mouse dendritic/interdigitating cell antibody (clone: MIDC8, 1 : 100 dilution, ABD serotec, Oxford, UK) were incubated together on thymus sections overnight at 4 °C. After washing three times with PBS, Alexa Fluor 488-conjugated donkey anti-goat IgG (H + L; Jackson, West Grove, PA, USA) and Alexa Fluor 594-conjugated donkey anti-rat IgG (H + L; Jackson) antibodies were added together and incubated for 30 min at room temperature. Nuclei were then labeled with DAPI (10 μg/ml). The slides were washed three times and photographed with a confocal laser scanning microscope (CLSM; Leica, Wetzlar, Germany).

Cell preparation, antibodies and flow cytometry analysis. The mice were killed and exsanguinated at the indicated dpi. The thymus, spleen and MLN were gently passed through a 200-μm nylon mesh, incubated in red blood cell lysis buffer (BD Biosciences, San Jose, CA, USA) and washed with PBS. Lung mononuclear cells were isolated as previously described. Briefly, the lungs were excised, minced and subsequently digested in DMEM (containing 0.1% collagenase I (Sigma-Aldrich, St. Louis, MO, USA) and 5% fetal calf serum) for 60 min at 37 °C on a rocking platform. The enzyme-digested lung tissues were also passed through 200-μm nylon and then washed with DMEM. The mononuclear cells were prepared by density gradient centrifugation with 40 and 70% Percoll (GE Healthcare, Buckinghamshire, UK). The cells were collected from the 40/70% Percoll interface and washed twice. Finally, the cells were counted by trypan blue exclusion using a hemocytometer.

For extracellular cell marker analysis, 10^6 cells were labeled with the following antibodies: mAbs against mouse CD3e-PerCP-CY5.5, CD4 (L3T4)-APC-H7 and CD8a-FITC. The $NP_{147-155}$ (TYQRTRALV) tetramer was synthesized by QuantoBio (Beijing, China) and used according to the manufacturer's instructions. Briefly, 10^6 cells were incubated with 5 μl of tetramer for 30 min at room temperature in a total volume of 0.1 ml and subsequently stained for cell markers at 4 °C for 30 min.

Intracellular staining of granzyme B, IFN-γ, Eomes, Foxp3 and perforin were performed as previously described.[47] Briefly, 10^6 thymocytes were cultured in DMEM (10% FCS) with GolgiPlug (BD Biosciences) to block the cellular secretion of cytokines for 5 h. The cells were then washed and stained with CD3e-PE-Cy7, CD4 (L3T4)-APC-H7, CD8a-FITC, DX5-PE, $\gamma\delta$TCR-APC, CD122-PE, CD44-PE-Cy7 or CD8a-alexa 647. Subsequently, the cells were incubated with Fix/Perm solution (BD Biosciences) at 4 °C for 20 min, and after washing with and diluting in Perm/Wash buffer (BD Biosciences), the cells were stained for intracellular cytokines (granzyme B-PE, IFN-γ-PerCP-CY5.5, Eomes-PE, Foxp3-Alexa 647 and perforin-APC) at 4 °C for 30 min. Finally, the cells were washed and analyzed on a FACSCanto II flow cytometer (BD Biosciences).

For apoptosis detection assay, 2×10^5 cells were firstly labeled with the following antibodies: mAbs against mouse CD4 (L3T4)-APC-H7 and CD8a-FITC. Staining of apoptotic cells in the thymus with annexin-V and PI was performed according to the manufacturer's instructions (BD Biosciences).

All fluorochrome-conjugated Abs were purchased from BD Biosciences or eBioscience (San Diego, CA, USA). The acquisition of the cell populations was performed on a FACSCanto II flow cytometer using BD FACSDiva software (BD Biosciences). The data were analyzed using FlowJo 7.6.1 software (Treestar, Ashland, OR, USA).

Cytokine and chemokine measurements in the thymus. For cytokine and chemokine measurements, the homogenized thymus was lysed in RIPA lysis buffer (Beyotime, Jiangsu, China), and the protein concentration was determined using the BCA assay (Beyotime). The samples were processed using the Bio-Plex mouse cytokine 23-Plex panel and the Th17 8-Plex panel arrays (Bio-Rad Laboratories, Hercules, CA, USA) and detected using the Bio-Plex Protein Array System (Bio-Rad Laboratories) according to the manufacturer's instructions. The concentrations were calculated by using the function: Relative concentration = cytokine concentration/total protein concentration.

RT-PCR and quantitative real-time PCR. RT-PCR was performed according to the manufacturer's instructions. Briefly, total RNA was isolated from homogenized thymus and lung tissues using Trizol reagent (Invitrogen, Grand Island, NY, USA), and cDNA was synthesized from RNA (1 μg) using random primers and the SuperScript III First Strand Synthesis System (Invitrogen).

Quantitative real-time PCR was used to detect virus HA, as described previously.[47] The primers for IFN-γ were as follows: sense 5′-TCAAGTGGCATAGA TGTGGAAGAA-3′ and antisense 5′-TGGCTCTGCAGGATTTTCATG-3′.[48] The primers for IL-7 were as follows: sense 5′-TCTGCTGCCTGTCACATCATC-3′ and antisense 5′-GGACATTGAATTCTTCACTGATATTCA-3′.[49] The primers for β-actin were as follows: sense 5′-AGAGGGAAATCGTGCGTGAC-3′ and antisense 5′-CAA TAGTGATGACCTGGCCGT-3′.[48] Real-time PCR was performed in a 20-μl volume (10 μl of 2 × SsoFast EVA Green supermix (Bio-Rad Laboratories), 1 μl of forward primer (10 μM), 1 μl of reverse primer (10 μM), 1 μl of cDNA and 7 μl of ddH_2O). The amplification products were detected using a C1000TM Quantitative Real-time PCR Thermal Cycler (Bio-Rad Laboratories). The reactions were initiated by incubation at 95 °C for 30 s, followed by 40 cycles of 95 °C for 10 s, 58 °C for 30 s and 72 °C for 5 s. The primer efficiency and specificity were demonstrated by the overlapping amplification profiles and the melting curves of equal quantities of cDNA, respectively. The relative expression values were normalized to the expression value of the housekeeping gene β-actin.

Determination of serum corticosterone level. Peripheral blood samples were obtained at 900 h from a venous incision at the tip of the tail ($n = 3$). Sera were then collected and stored at -80 °C. The concentrations of corticosterone were assayed using an ELISA kit (Hermes Criterion Biotechnology, Elixir, Vancouver, BC, Canada) according to the manufacturer's instructions.

Antiviral activity of peramivir. After infected intranasally with virus (10^6 $TCID_{50}$ in 50 μl), peramivir was subsequently administered intraperitoneally at a dose of 40 mg/kg daily for 5 days, with PBS as control.[50] Thymus weight, histology and flow cytometry were measured as described above.

Neutralization of IFN-γ *in vivo*. For neutralizing endogenous IFN-γ, mice were either injected intraperitoneally with rat anti-mouse IFN-γ monoclonal antibody (mAb; R4-6A2; eBioscience) or with PBS as control. Antibody (0.25 mg per mouse) was administered starting on day 1 before virus infection.[51]

Statistical analysis. The data were analyzed using GraphPad Software (GraphPad Prism 5, GraphPad Software, Inc., La Jolla, CA, USA) and are presented as the mean ± S.D. Statistically significant differences were assessed using an unpaired two-tailed Student's *t*-test. *P*-values < 0.05 were considered statistically significant.

Conflict of Interest

The authors declare no conflict of interest.

Acknowledgements. We thank Lan Huang and Qi Lv for technical support. We also appreciate Professor ChengYu Jiang for carefully editing the manuscript. This work was supported by grants from the National Natural Science Foundation of China (grant number 81070005/H0104, 81030032/H19, 81271840 and 81373114).

1. Centers for Disease Control and Prevention (CDC). Swine influenza A (H1N1) infection in two children–Southern California March-April 2009. *MMWR Morb Mortal Wkly Rep* 2009; **58**: 400–402.
2. Chowell G, Bertozzi SM, Colchero MA, Lopez-Gatell H, Alpuche-Aranda C, Hernandez M *et al.* Severe respiratory disease concurrent with the circulation of H1N1 influenza. *N Engl J Med* 2009; **361**: 674–679.
3. Kumar A, Zarychanski R, Pinto R, Cook DJ, Marshall J, Lacroix J *et al.* Critically ill patients with 2009 influenza A(H1N1) infection in Canada. *JAMA* 2009; **302**: 1872–1879.
4. Perez-Padilla R, de la Rosa-Zamboni D, Ponce de Leon S, Hernandez M, Quinones-Falconi F, Bautista E *et al.* Pneumonia and respiratory failure from swine-origin influenza A (H1N1) in Mexico. *N Engl J Med* 2009; **361**: 680–689.
5. Centers for Disease Control and Prevention (CDC). Update: novel influenza A (H1N1) virus infection - Mexico, March-May, 2009. *MMWR Morb Mortal Wkly Rep* 2009; **58**: 585–589.
6. Itoh Y, Shinya K, Kiso M, Watanabe T, Sakoda Y, Hatta M *et al. In vitro* and *in vivo* characterization of new swine-origin H1N1 influenza viruses. *Nature* 2009; **460**: 1021–1025.
7. Tran TH, Nguyen TL, Nguyen TD, Luong TS, Pham PM, Nguyen v V *et al.* Avian influenza A (H5N1) in 10 patients in Vietnam. *N Engl J Med* 2004; **350**: 1179–1188.
8. Maines TR, Szretter KJ, Perrone L, Belser JA, Bright RA, Zeng H *et al.* Pathogenesis of emerging avian influenza viruses in mammals and the host innate immune response. *Immunol Rev* 2008; **225**: 68–84.
9. Cao B, Li XW, Mao Y, Wang J, Lu HZ, Chen YS *et al.* Clinical features of the initial cases of 2009 pandemic influenza A (H1N1) virus infection in China. *N Engl J Med* 2009; **361**: 2507–2517.
10. Cunha BA, Pherez FM, Schoch P. Diagnostic importance of relative lymphopenia as a marker of swine influenza (H1N1) in adults. *Clin Infect Dis* 2009; **49**: 1454–1456.
11. Savino W. The thymus is a common target organ in infectious diseases. *PLoS Pathog* 2006; **2**: e62.
12. Hale JS, Boursalian TE, Turk GL, Fink PJ. Thymic output in aged mice. *Proc Natl Acad Sci USA* 2006; **103**: 8447–8452.
13. Vogel AB, Haasbach E, Reiling SJ, Droebner K, Klingel K, Planz O. Highly pathogenic influenza virus infection of the thymus interferes with T lymphocyte development. *J Immunol* 2010; **185**: 4824–4834.

14. Tian J, Qi W, Li X, He J, Jiao P, Zhang C *et al.* A single E627K mutation in the PB2 protein of H9N2 avian influenza virus increases virulence by inducing higher glucocorticoids (GCs) level. *PLoS One* 2012; **7**: e38233.
15. Surh CD, Sprent J. Homeostasis of naive and memory T cells. *Immunity* 2008; **29**: 848–862.
16. Lee YJ, Jameson SC, Hogquist KA. Alternative memory in the CD8 T cell lineage. *Trends Immunol* 2011; **32**: 50–56.
17. Berg LJ. Signalling through TEC kinases regulates conventional versus innate CD8(+) T-cell development. *Nat Rev Immunol* 2007; **7**: 479–485.
18. Weinreich MA, Odumade OA, Jameson SC, Hogquist KA. T cells expressing the transcription factor PLZF regulate the development of memory-like CD8+ T cells. *Nat Immunol* 2010; **11**: 709–716.
19. Rafei M, Hardy MP, Williams P, Vanegas JR, Forner KA, Dulude G *et al.* Development and function of innate polyclonal TCRalphabeta+ CD8+ thymocytes. *J Immunol* 2011; **187**: 3133–3144.
20. Hagau N, Slavcovici A, Gonganau DN, Oltean S, Dirzu DS, Brezoszki ES *et al.* Clinical aspects and cytokine response in severe H1N1 influenza A virus infection. *Crit Care* 2010; **14**: R203.
21. Robertson AM, Bird CC, Waddell AW, Currie AR. Morphological aspects of glucocorticoid-induced cell death in human lymphoblastoid cells. *J Pathol* 1978; **126**: 181–187.
22. Thompson BT. Glucocorticoids and acute lung injury. *Crit Care Med* 2003; **31**(4 Suppl): S253–S257.
23. von Freeden-Jeffry U, Vieira P, Lucian LA, McNeil T, Burdach SE, Murray R. Lymphopenia in interleukin (IL)-7 gene-deleted mice identifies IL-7 as a nonredundant cytokine. *J Exp Med* 1995; **181**: 1519–1526.
24. Park JH, Adoro S, Guinter T, Erman B, Alag AS, Catalfamo M *et al.* Signaling by intrathymic cytokines, not T cell antigen receptors, specifies CD8 lineage choice and promotes the differentiation of cytotoxic-lineage T cells. *Nat Immunol* 2010; **11**: 257–264.
25. Yellen-Shaw AJ, Eisenlohr LC. Regulation of class I-restricted epitope processing by local or distal flanking sequence. *J Immunol* 1997; **158**: 1727–1733.
26. Gordon SM, Carty SA, Kim JS, Zou T, Smith-Garvin J, Alonzo ES *et al.* Requirements for eomesodermin and promyelocytic leukemia zinc finger in the development of innate-like CD8+ T cells. *J Immunol* 2011; **186**: 4573–4578.
27. Wyde PR, Couch RB, Mackler BF, Cate TR, Levy BM. Effects of low- and high-passage influenza virus infection in normal and nude mice. *Infect Immun* 1977; **15**: 221–229.
28. Savino W, Dardenne M, Marche C, Trophilme D, Dupuy JM, Pekovic D *et al.* Thymic epithelium in AIDS. An immunohistologic study. *Am J Pathol* 1986; **122**: 302–307.
29. Souto PC, Brito VN, Gameiro J, da Cruz-Hofling MA, Verinaud L. Programmed cell death in thymus during experimental paracoccidioidomycosis. *Med Microbiol Immunol* 2003; **192**: 225–229.
30. Perez AR, Roggero E, Nicora A, Palazzi J, Besedovsky HO, Del Rey A *et al.* Thymus atrophy during *Trypanosoma cruzi* infection is caused by an immuno-endocrine imbalance. *Brain Behav Immun* 2007; **21**: 890–900.
31. Lynch HE, Goldberg GL, Chidgey A, Van den Brink MR, Boyd R, Sempowski GD. Thymic involution and immune reconstitution. *Trends Immunol* 2009; **30**: 366–373.
32. Francelin C, Paulino LC, Gameiro J, Verinaud L. Effects of Plasmodium berghei on thymus: high levels of apoptosis and premature egress of CD4(+)CD8(+) thymocytes in experimentally infected mice. *Immunobiology* 2011; **216**: 1148–1154.
33. Borges M, Barreira-Silva P, Florido M, Jordan MB, Correia-Neves M, Appelberg R. Molecular and cellular mechanisms of Mycobacterium avium-induced thymic atrophy. *J Immunol* 2012; **189**: 3600–3608.
34. Nascimbeni M, Pol S, Saunier B. Distinct CD4+ CD8+ double-positive T cells in the blood and liver of patients during chronic hepatitis B and C. *PLoS One* 2011; **6**: e20145.
35. Wang D, Muller N, McPherson KG, Reichardt HM. Glucocorticoids engage different signal transduction pathways to induce apoptosis in thymocytes and mature T cells. *J Immunol* 2006; **176**: 1695–1702.
36. Lepletier A, de Frias Carvalho V, Morrot A, Savino W. Thymic atrophy in acute experimental Chagas disease is associated with an imbalance of stress hormones. *Ann N Y Acad Sci* 2012; **1262**: 45–50.
37. Chen W, Kuolee R, Austin JW, Shen H, Che Y, Conlan JW. Low dose aerosol infection of mice with virulent type A *Francisella tularensis* induces severe thymus atrophy and CD4+CD8+ thymocyte depletion. *Microb Pathog* 2005; **39**: 189–196.
38. Fayad R, Sennello JA, Kim SH, Pini M, Dinarello CA, Fantuzzi G. Induction of thymocyte apoptosis by systemic administration of concanavalin A in mice: role of TNF-alpha, IFN-gamma and glucocorticoids. *Eur J Immunol* 2005; **35**: 2304–2312.
39. Papadopoulou AS, Dooley J, Linterman MA, Pierson W, Ucar O, Kyewski B *et al.* The thymic epithelial microRNA network elevates the threshold for infection-associated thymic involution via miR-29a mediated suppression of the IFN-alpha receptor. *Nat Immunol* 2012; **13**: 181–187.
40. Deobagkar-Lele M, Chacko SK, Victor ES, Kadthur JC, Nandi D. Interferon-gamma- and glucocorticoid-mediated pathways synergize to enhance death of CD4(+) CD8(+) thymocytes during Salmonella enterica serovar Typhimurium infection. *Immunology* 2013; **138**: 307–321.
41. Bonasio R, Scimone ML, Schaerli P, Grabie N, Lichtman AH, von Andrian UH. Clonal deletion of thymocytes by circulating dendritic cells homing to the thymus. *Nat Immunol* 2006; **7**: 1092–1100.
42. Hao X, Kim TS, Braciale TJ. Differential response of respiratory dendritic cell subsets to influenza virus infection. *J Virol* 2008; **82**: 4908–4919.
43. Betts RJ, Prabhu N, Ho AW, Lew FC, Hutchinson PE, Rotzschke O *et al.* Influenza A virus infection results in a robust, antigen-responsive, and widely disseminated Foxp3+ regulatory T cell response. *J Virol* 2012; **86**: 2817–2825.
44. Sanchez AM, Zhu J, Huang X, Yang Y. The development and function of memory regulatory T cells after acute viral infections. *J Immunol* 2012; **189**: 2805–2814.
45. Bedoya F, Cheng GS, Leibow A, Zakhary N, Weissler K, Garcia V *et al.* Viral antigen induces differentiation of Foxp3+ natural regulatory T cells in influenza virus-infected mice. *J Immunol* 2013; **190**: 6115–6125.
46. Xu L, Bao L, Zhou J, Wang D, Deng W, Lv Q *et al.* Genomic polymorphism of the pandemic A (H1N1) influenza viruses correlates with viral replication, virulence, and pathogenicity in vitro and in vivo. *PLoS One* 2011; **6**: e20698.
47. Dawood FS, Iuliano AD, Reed C, Meltzer MI, Shay DK, Cheng PY *et al.* Estimated global mortality associated with the first 12 months of 2009 pandemic influenza A H1N1 virus circulation: a modelling study. *Lancet Infect Dis* 2012; **12**: 687–695.
48. Giulietti A, Overbergh L, Valckx D, Decallonne B, Bouillon R, Mathieu C. An overview of real-time quantitative PCR: applications to quantify cytokine gene expression. *Methods* 2001; **25**: 386–401.
49. Ortman CL, Dittmar KA, Witte PL, Le PT. Molecular characterization of the mouse involuted thymus: aberrations in expression of transcription regulators in thymocyte and epithelial compartments. *Int Immunol* 2002; **14**: 813–822.
50. Kitano M, Kodama M, Itoh Y, Kanazu T, Kobayashi M, Yoshida R *et al.* Efficacy of repeated intravenous injection of peramivir against influenza A (H1N1) 2009 virus infection in immunosuppressed mice. *Antimicrob Agents Chemother* 2013; **57**: 2286–2294.
51. Wang C, Xiao M, Liu X, Ni C, Liu J, Erben U *et al.* IFN-gamma-mediated downregulation of LXA4 is necessary for the maintenance of nonresolving inflammation and papilloma persistence. *Cancer Res* 2013; **73**: 1742–1751.

Supplementary Information accompanies this paper on Cell Death and Disease website (http://www.nature.com/cddis)